Ratio of the Second and Third Turbulent Moments in the Urban Boundary Layer of the Atmosphere Using the Example of Data from the Moscow State University Eddy Covariance Tower

Article *in* Izvestiya Atmospheric and Oceanic Physics · August 2023

DOI: 10.1134/S0001433823040151

CITATIONS
0

READS
32

7 authors, including:

Ilya Drozd
A.M. Obukhov Institute of Atmospheric Physics
9 PUBLICATIONS **20** CITATIONS
SEE PROFILE

Arseny Yurevich Artamonov
A.M. Obukhov Institute of Atmospheric Physics Russian Academy of Sciences
43 PUBLICATIONS **179** CITATIONS
SEE PROFILE

Kirill Barskov
A.M. Obukhov Institute of Atmospheric Physics
14 PUBLICATIONS **69** CITATIONS
SEE PROFILE

Alexander Gavrikov
P.P. Shirshov Institute of Oceanology
47 PUBLICATIONS **225** CITATIONS
SEE PROFILE

ISSN 0001-4338, Izvestiya, Atmospheric and Oceanic Physics, 2023, Vol. 59, No. 4, pp. 443–455. © Pleiades Publishing, Ltd., 2023.
Russian Text © The Author(s), 2023, published in Izvestiya Rossiiskoi Akademii Nauk, Fizika Atmosfery i Okeana, 2023, Vol. 59, No. 4, pp. 509–522.

Ratio of the Second and Third Turbulent Moments in the Urban Boundary Layer of the Atmosphere Using the Example of Data from the Moscow State University Eddy Covariance Tower[1]

I. D. Drozd[a, b, c, *], A. Yu. Artamonov[b], K. V. Barskov[b], A. V. Gavrikov[b, d], A. D. Pashkin[b], I. A. Repina[b, c, e], and V. M. Stepanenko[a, b, c, e]

[a] *Faculty of Geography, Moscow State University, Moscow, 119234 Russia*
[b] *Obukhov Institute of Atmospheric Physics, Russian Academy of Sciences, Moscow, 119017 Russia*
[c] *Research Computing Center, Moscow State University, Moscow, 119234 Russia*
[d] *Shirshov Institute of Oceanology, Russian Academy of Sciences, Moscow, 117218 Russia*
[e] *Moscow Center for Fundamental and Applied Mathematics, Moscow, 119234 Russia*
**e-mail: drozdil.msu@gmail.com*

Received February 6, 2023; revised April 21, 2023; accepted April 26, 2023

Abstract—In this paper, we test the hypothesis about the presence of a diagnostic relation between the second and third moments of hydrodynamic quantities c_1 and c_2 in the atmospheric boundary layer above a geometrically complex surface: $\overline{w' c_1' c_2'} = CS_{c_1}\sigma_{c_1}\overline{w' c_2'}$. To test this relation, a 7-month series of high-frequency measurements on an eddy covariance tower installed at the Meteorological Observatory (MO) at Moscow State University is used. The optimal methods for analyzing the reliability of the dependence are evaluated based on the statistical distribution of third moments. A statistically valid estimate of the validity of the tested hypothesis is obtained on a large series of data under the conditions of the urban underlying surface for the first time. The effect of stratification conditions and the nature of the underlying surface in the area of flux formation on the fulfillment of the relation is studied. The relation is established to be valid in 80% of cases for third moments $\overline{w' w' T'}$, $\overline{w' T' T'}$, $\overline{w' u' u'}$ and $\overline{w' v' v'}$.

Keywords: atmospheric boundary layer, urban surface, eddy covariance method, turbulent fluxes, third moments

DOI: 10.1134/S0001433823040151

INTRODUCTION

The mathematical description of turbulent processes in the boundary layer of the atmosphere is an important component for successfully solving problems of numerically predicting its dynamics. These processes are the main mechanism for the exchange of energy and mass between the atmosphere and the surface. To calculate turbulent flows in a horizontally statistically uniform surface layer, the Monin–Obukhov similarity theory (MOST) (Monin and Obukhov, 1954) became widely used, the generalization to the case of a flow over an inhomogeneous surface of which is still not practically developed. The use of MOST is limited to the lower layer of the atmosphere above a homogeneous surface, in which the stability parameter is $|z/L| \le 1$–2 (Monin and Yaglom, 1965; Kaimal and Finnigan 1994; Wyngaard 2010). Under these conditions, the statistical characteristics of meteorological fields can depend only on the measurement height.

The measurement data show that, in a heterogeneous landscape (a glade, a lake surrounded by forests, and urban and mountain canyons), at the levels of standard measurements, there is a rapid change in the heat and momentum fluxes with height that does not make it possible in the general case to associate the fluxes measured at a certain height with the fluxes at surfaces. Despite the idealization of the conditions of MOST, this theory, together with Kolmogorov's theory of the existence of an inertial interval in the spectra of the velocity components, is widely used to estimate the fluxes of momentum, heat and moisture, and the transport of impurities in the surface layer in weather and climate forecast models both over land and above

[1] This paper was prepared based on an oral report presented at the IV All-Russian Conference with international participation of "Turbulence, Atmospheric and Climate Dynamics" dedicated to the memory of Academician A.M. Obukhov (Moscow, November 22–24, 2022).

the sea. In the presence of horizontal and vertical gradients of statistical moments of meteorological quantities (in particular, fluxes), the use of MOST must lead to errors, the level of which has not been sufficiently studied to date.

Difficulties in the applicability of MOST over inhomogeneous landscapes are primarily due to the fact that, in addition to local turbulent mixing caused by high-frequency turbulence, nonlocal processes caused by the inhomogeneity of the generation of turbulent motions and various mesoscale circulations are added here. Under certain conditions, MOST is also applicable over an inhomogeneous surface. However, in this case, a more generalized approach is needed to calculate the characteristics of atmospheric turbulence, which may include, among other things, classical MOST as a special case (Johansson et al., 2001; Wilson, 2008). There were attempts to include new independent dimensionless groups in the similarity functions (Grachev et al., 2015, 2018) or introduce new empirical scales (Barskov et al., 2018), as well as to develop a similarity theory that takes into account both vertical and horizontal scales of turbulent flows (Tong and Nguen, 2015; Stiperski and Calaf, 2022), but these studies were more of a private nature.

Experimental data are needed to study the statistical characteristics of the turbulence of the atmospheric boundary layer in urban areas. The regularities may in the future make it possible to generalize MOST for the use under conditions of a heterogeneous landscape.

In this paper, we present the results of a study of the mechanisms of turbulent exchange over a geometrically complex urban surface according to the data of an eddy covariance tower installed at the Meteorological Observatory (MO), Moscow State University.

ALGEBRAIC RELATION OF THE SECOND AND THIRD MOMENTS IN THE PRESENCE OF COHERENT STRUCTURES

Turbulent closures of the second order that use an algebraic relation between the second and third moments, which is obtained under the assumption of the presence of coherent structures, were first proposed in theoretical studies of the convective boundary layer (Abdella and McFarlane, 1997; Zilitinkevich et al., 1999; Barskov et al., 2022). According to the hypothesis proposed by these authors, at the predominant contribution of large-scale eddies to turbulent flows, the second and third moments including a scalar quantity, for example, temperature, are related by algebraic relations:

$$\overline{w'w'\theta'} = CS_w\sigma_w\overline{w'\theta'}, \quad (1)$$

$$\overline{w'\theta'\theta'} = CS_\theta\sigma_\theta\overline{w'\theta'}, \quad (2)$$

where $S_c = \dfrac{\overline{c'^3}}{\overline{c'^2}^{3/2}}$ is the asymmetry coefficient, $\sigma_c = \left(\overline{c'^2}\right)^{1/2}$ is the standard deviation of $c = w, \theta, w$ is the vertical component of the wind velocity, θ is the potential temperature, and C is the dimensionless constant that is ~1. The derivation of formulas (1) and (2) is considered in detail in (Zilitinkevich et al., 1999) and is not presented here. Hypothesis (1) can be written with the replacement of temperature by any other scalar value (humidity, concentration of gaseous or aerosol impurities, etc.) or the horizontal velocity component of $\theta \to u_i$, $i = 1,2$, since formula (1) remains invariant with respect to the rotation of the horizontal axes of the Cartesian system. A hypothesis similar to (2) regarding the horizontal components u_i and, u_j, $i, j = 1,2$; $u_1 = u$, $u_2 = v$ must also satisfy the invariance to the rotation of the horizontal coordinate axes. For this, it is sufficient to accept the equality

$$\overline{w'u_i'u_j'} = C\frac{\overline{u_k'u_n'u_i'}}{\overline{u_k'u_n'}}\overline{w'u_j'}, \quad (3)$$

where the i, j, k, n subscripts take the value of 1 or 2, while the summation over repeated indices on the right side is optional. In the particular case of $i = j = k = n$, we obtain a similar (1), (2) expression:

$$\overline{w'u_i'u_i'} = C\frac{\overline{u_i'^3}}{\overline{u_i'^2}^{3/2}}\left(\overline{u_i'^2}\right)^{1/2}\overline{w'u_i'}. \quad (4)$$

In (Zilitinkevich et al., 1999), hypothesis (1), (2) for temperature was successfully tested on the data of eddy-resolving modeling (Large Eddy Simulation or LES) of the convective boundary layer.

Equations (1), (2) are obtained strictly in the presence of ordered ascending and descending branches of coherent structures. However, these structures can develop not only in the convective boundary layer, but also over large obstacles (roughness elements) (Kadivar et al., 2021), a complex combination of which is, for example, an urbanized surface. Thus, it can be assumed that, in the roughness layer above the urban surface, the above relations must be satisfied not only in unstable, but also in indifferent and stable stratification (Zilitinkevich, 2002).

Despite the fact that algebraic relations (1), (2) were proposed more than 20 years ago, no studies were apparently carried out to test them on a long series of measurement data. For example, in (Barskov et al., 2019), hypothesis (1) was tested based on measurement data over a lake near the forest edge over a period of about a week. It was found that, in the presence of large elements of geometric inhomogeneity of the sur-

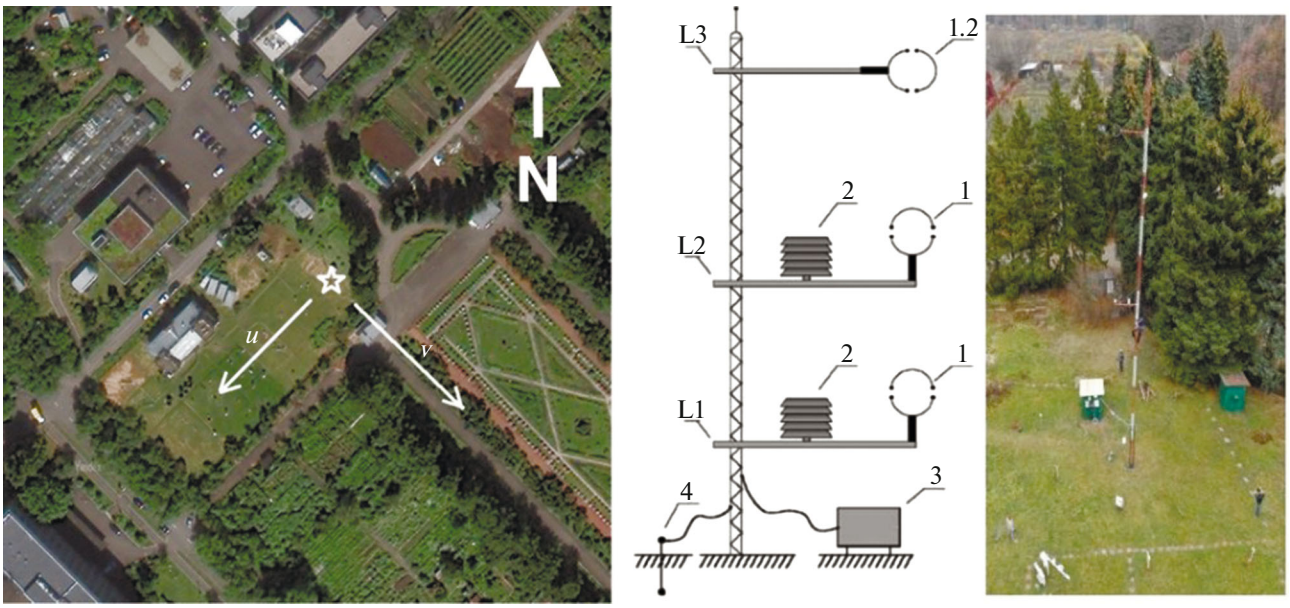

Fig. 1. Location of an eddy covariance tower (marked with a white star) at the Moscow State University MO and the directions of the horizontal axes of the anemometers (left). Photograph of an eddy covariance tower and a diagram of the arrangement of instruments on an eddy covariance tower: measurement levels L1, L2, and L3 at 2.2, 11.1, and 18.8 m; uSonic-3 Scientific acoustic anemometers at 2.2 m and 11.1 m, (1) anemometer uSonic-3 of class A at 18.8 m; (2) humidity and temperature sensors HMP155 from Vaisala; (3) data collection system; and (4) ground loop (right) (Artamonov et al., 2019).

face on the windward side, the heat flux is better described by formula (1) while, in the absence of such elements, by the MOST. In (Pashkin et al., 2021), the statistical distribution of the dimensionless constant in Eq. (1) for urban conditions is considered using the example of selective short series of measurements, and the assumption that $C \sim 1$ is convincingly confirmed. In (Barskov et al., 2022), the distribution of third moments over various types of heterogeneous underlying surface, including urban one, are compared.

In the present study, we test the hypothesis for city conditions based on a long (7 months) continuous series of high-frequency measurements applied to the vertical heat flux (1), (2), as well as to the momentum component fluxes (4) as part of the analysis of the statistical characteristics of the boundary layer turbulence according to the data of an eddy covariance tower installed at the MO at Moscow State University. More specifically, we exam the hypothesis about the relation between the second and third turbulent moments (the so-called Zilitinkevich hypothesis) under various conditions of stratification and the nature of the underlying urban surface.

MEASURING COMPLEX AND DATA PROCESSING

The measuring complex of an eddy covariance tower installed at the MO at Moscow State University includes measurement levels at heights of 2.2, 11.1, and 18.8 m (Artamonov et al., 2019; Drozd et al., 2022b). Using METEK uSonic-3 Scientific (2.2 and 11.1 m) and uSonic-3 class A (18.8 m) acoustic anemometers, three components of the wind velocity and acoustic temperature are measured with a frequency of 20 Hz and an accuracy of 0.1 m/s and 0.1°C, respectively (Fig. 1). In this study, the difference between the acoustic and virtual temperatures is neglected since, for the data used, it averages 0.01°C, which is an order of magnitude lower than the accuracy of the acoustic anemometers.

Before their analysis, the data are first preprocessed. Initially, the data series with allowance for the characteristics of each measuring device are brought to a general form, corrective amendments are made, and the axes of the devices are rotated. Next, the data from the three measuring levels enter the subsequent stage of processing to be prepared in the same units of measurement and to have the same axes (Fig. 1). Then, peak values are filtered, the deviation from the average of which exceeds three and a half standard deviations over a 20-min averaging period and, for vertical wind velocity, five standard deviations, while if the deviations exceed the threshold values for three or more measurements in a row, such peaks are considered significant and are not removed. If no more than 20% of the values are missing in the processed 20 min data series, it proceeds to the next stage of processing; otherwise, all 20 min are not taken into account. The next stage of processing is the restoration of missing data. For this, a method based on the Gaussian distribution of correlated values before and after the gap is used

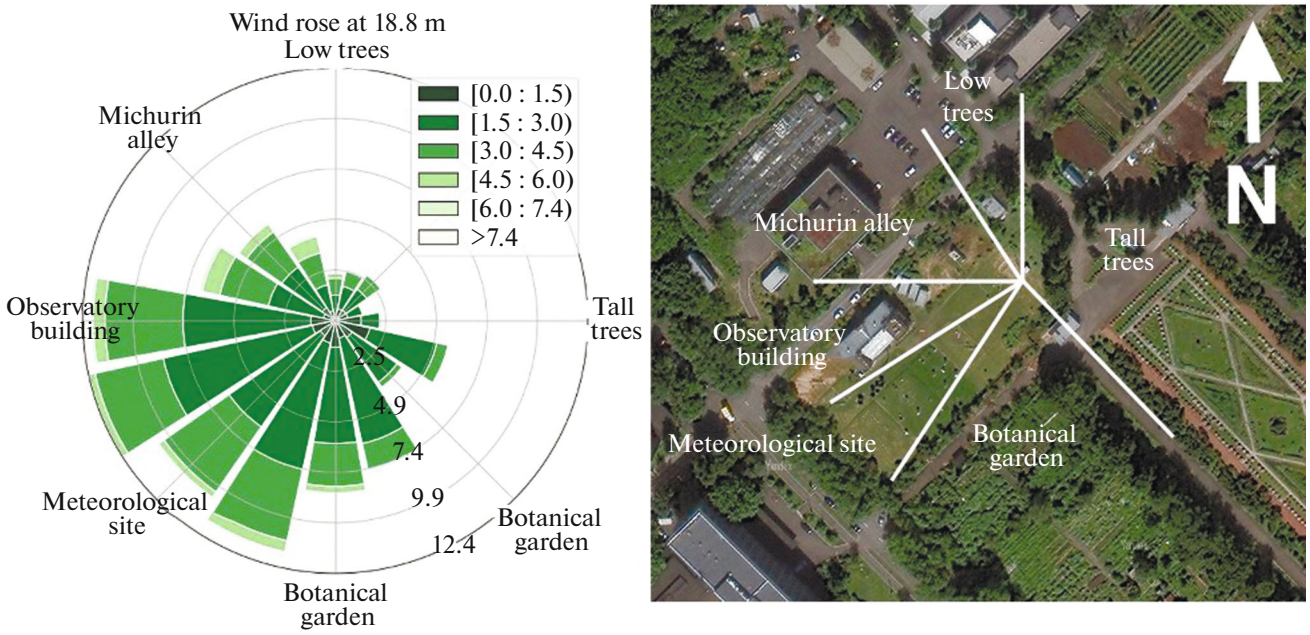

Fig. 2. Wind rose of a Moscow State University eddy covariance tower from November 1, 2019, to May 31, 2020, at a height of 18.8 m (left); wind direction sectors identified by the criterion of relative uniformity of the underlying surface (right).

(Drozd et al., 2022a), while gaps longer than 1 min were not filled. At the final stage of processing, detrending and calculation of average values over 20 min is carried out. Next, the second and third moments of velocity and temperature and the quantities derived from them are calculated.

To test the hypotheses (1), (2), and (4), a mast data array from November 1, 2019, to May 31, 2020, was selected, while data for the period from 14:00 November 3, 2019, to 15:00 November 9, 2019, and from 02:00 December 27, 2019, to 03:00 December 29, 2019 (Moscow time), are absent due to technical malfunctions of the mast at this time. Here, we demonstrate the results from measurements at a height of 11.1 and 18.8 m, since these levels are located in the upper part of the roughness layer (comparable to the height of nearby buildings and tall trees) and are representative of the urban surface layer. The measurements for the indicated period were divided into cases with different wind directions (Fig. 2). The boundaries of the sectors shown in Fig. 2 were identified according to the nature of the underlying surface and are shown in Table 1.

To consider the effect of stratification conditions on hypotheses (1), (2), and (4), the analyzed data set was also divided by stratification types. To determine the stratification conditions, the stability parameter was used:

$$\xi = \frac{z}{L} = -\frac{zgu_2\varkappa\overline{w'T'}}{\overline{T}\left(\overline{w'u'}^2 + \overline{w'v'}^2\right)^{3/4}}, \quad (5)$$

where z is the measurement height, L is the Obukhov scale, $\overline{T}$ is the average temperature, g is the acceleration of gravity, $\varkappa$ is the Karman constant, $\overline{w'T'}$ is the vertical heat flux, and $\overline{w'v'}$ are the components of the vertical momentum flux. Cases with $\xi < -0.01$ were assigned to unstable stratification, $-0.01 \le \xi \le 0.01$ to indifferent stratification, and $\xi > 0.01$ to stable stratification.

RESULTS AND DISCUSSION

Alongside third moments $\overline{w'w'T'}$, $\overline{w'T'T'}$, $\overline{w'u'u'}$, $\overline{w'v'v'}$, calculated from the measurement data, estimates of third moments $\overline{w'w'T'}_{th}$, $\overline{w'T'T'}_{th}$, $\overline{w'u'u'}_{th}$, $\overline{w'v'v'}_{th}$, where $\overline{w'c_1'c_2'}_{th} \equiv S_{c_1}\left(\overline{c_i'^2}\right)^{1/2}\overline{w'c_2'}$ (here, $c_1 = w$, $c_2 = T$ or $c_1 = c_2 = w, T, u, v$), hereinafter

Table 1. Selected sectors around a Moscow State University eddy covariance tower. Sector boundaries are given in degrees relative to the north of the instrument (azimuth is 135°)

	Botanical garden	Meteorological site	Observatory building	Michurin alley	Low trees	Tall trees
Sector boundaries, °	0–70	70–100	100–130	130–180	180–245	245–360

referred to as *theoretical third moments* and denoted as the third moments with the subscript *th*, were obtained. Using the introduced notation, hypotheses (1), (2), and (4) take the form

$$\overline{w'c_1'c_2'} = C\overline{w'c_1'c_2'}_{th}. \quad (6)$$

Equation (6) shows that the relation of measured and theoretical third moments must be described by the linear regression with the zero free coefficient and angular slope of ≈ 1 according to the Zilitinkevich hypothesis. Applying Student's t-test and evaluating the p significance level for the null hypothesis slope = 1, quantitative estimates of the confirmation of the hypothesis were obtained. It is accepted that the hypothesis is statistically justified if the value is $p > 0.05$. To estimate the significance of the results, 95% confidence intervals are given for the calculated values of the regression slope and determination coefficients. Examples of estimates obtained for heights of 11.1 and 18.8 m in different sectors for various third moments are shown in Fig. 3.

Along with obtaining numerical characteristics of the reliability of the hypothesis, the scatterplots shown in Fig. 3 make it possible to visually estimate the nature of the distribution of the measured third moments relative to the theoretical ones. For third moments $\overline{w'w'T'}$, the following regularities in the mutual distribution are valid. At unstable stratification, the greatest scatter of both measured and theoretical values is observed, with most of the points lying in the 3rd quarter of the plot (negative $\overline{w'w'T'}$ and $\overline{w'w'T'}_{th}$). For stable stratification, the scatter of third moments is an order of magnitude smaller, and most of the points are in the 1st quarter of the plot (positive $\overline{w'w'T'}$ and $\overline{w'w'T'}_{th}$). The amplitude of the scatter of points for neutral stratification is comparable to the amplitude for stable stratification, and the values of the third moments are densely grouped on both sides of zero. All stratification conditions are characterized by a greater value scatter of $\overline{w'w'T'}$, than $\overline{w'w'T'}_{th}$, i.e., the point clouds are more elongated along the y axis, which is why the slope of the regression in most cases is greater than unity. This is most pronounced at neutral stratification, while the coefficient of determination for the subsample with neutral stratification is the lowest.

The values of third moments $\overline{w'T'T'}$ and $\overline{w'T'T'}_{th}$ are distributed with less scatter than those of third moments $\overline{w'w'T'}$. The greatest scatter of points is typical for conditions of unstable stratification, and the cloud of points is shifted to the right half of the plot (positive $\overline{w'T'T'}_{th}$). Point clouds for stable and neutral stratification are densely grouped around zero. For unstable and stable stratification, a larger value scatter is characteristic of $\overline{w'T'T'}_{th}$, than $\overline{w'T'T'}$, i.e., point clouds are more elongated along the abscissa axis, so the regression slope in most cases is less than unity. At nondifferential stratification, like for the relation of $\overline{w'w'T'}$ and $\overline{w'w'T'}_{th}$, there is a tendency to overestimate the regression slope ($C > 1$) due to the elongation of the point cloud along the y axis.

The distribution of third moments $\overline{w'u'u'}$ with respect to $\overline{w'u'u'}_{th}$ has a pronounced linear component and does not depend on the stratification conditions. The vast majority of points are in the 3rd quadrant (negative $\overline{w'u'u'}$ and $\overline{w'u'u'}_{th}$), and the amplitude of the point scatter is an order of magnitude higher than that for third moments $\overline{w'w'T'}$. All stratification conditions are characterized by high determination coefficients, and regression coefficients are close to unity. On the other hand, the distribution of third moments $\overline{w'v'v'}$ relative to $\overline{w'v'v'}_{th}$,is poorly described by the linear regression. The amplitude of the value scatter of $\overline{w'v'v'}$ and $\overline{w'v'v'}_{th}$ for all stratification conditions is comparable to that of third moments $\overline{w'u'u'}$, however, the point cloud for most of the considered sectors does not have a pronounced trend in the distribution and is quasi-uniformly distributed around zero. The low determination coefficients under all stratification conditions also indicate the low descriptive ability of the linear model for this type of distributions. The exception is the Tall Trees sector at 11.1 m, where there is a slight linear trend in the distribution of third moments $\overline{w'v'v'}$.

The angular coefficients (C) and determination coefficients (R^2) obtained during the regression analysis are shown in Figs. 4 (18.8 m) and 5 (11.1 m). Hypotheses (1–2, and 4) were tested on data from two height levels on subsamples of six sectors (Table 1) and in all directions at once, as well as for three stratification conditions. Thus, for third moments $\overline{w'w'T'}$, $\overline{w'T'T'}$, $\overline{w'u'u'}$ and $\overline{w'v'v'}$ 168 estimates of C and R^2, each based on a range of data from 310 to 5519 values, were obtained in total. Hypotheses (1), (2), and (4) were considered confirmed if the value of the C coefficient or part of its confidence interval is in the range from 0.5 to 2. Based on the estimates for third moments $\overline{w'w'T'}$ and $\overline{w'T'T'}$, a significant dependence of the distribution of C and R^2 values on stratification was revealed. Thus, in 79% of cases, C values at neutral stratification turned out to be higher than C values under conditions of stable or unstable stratification, while 50% of C values overestimated relative to other cases of stratification were above the upper limit

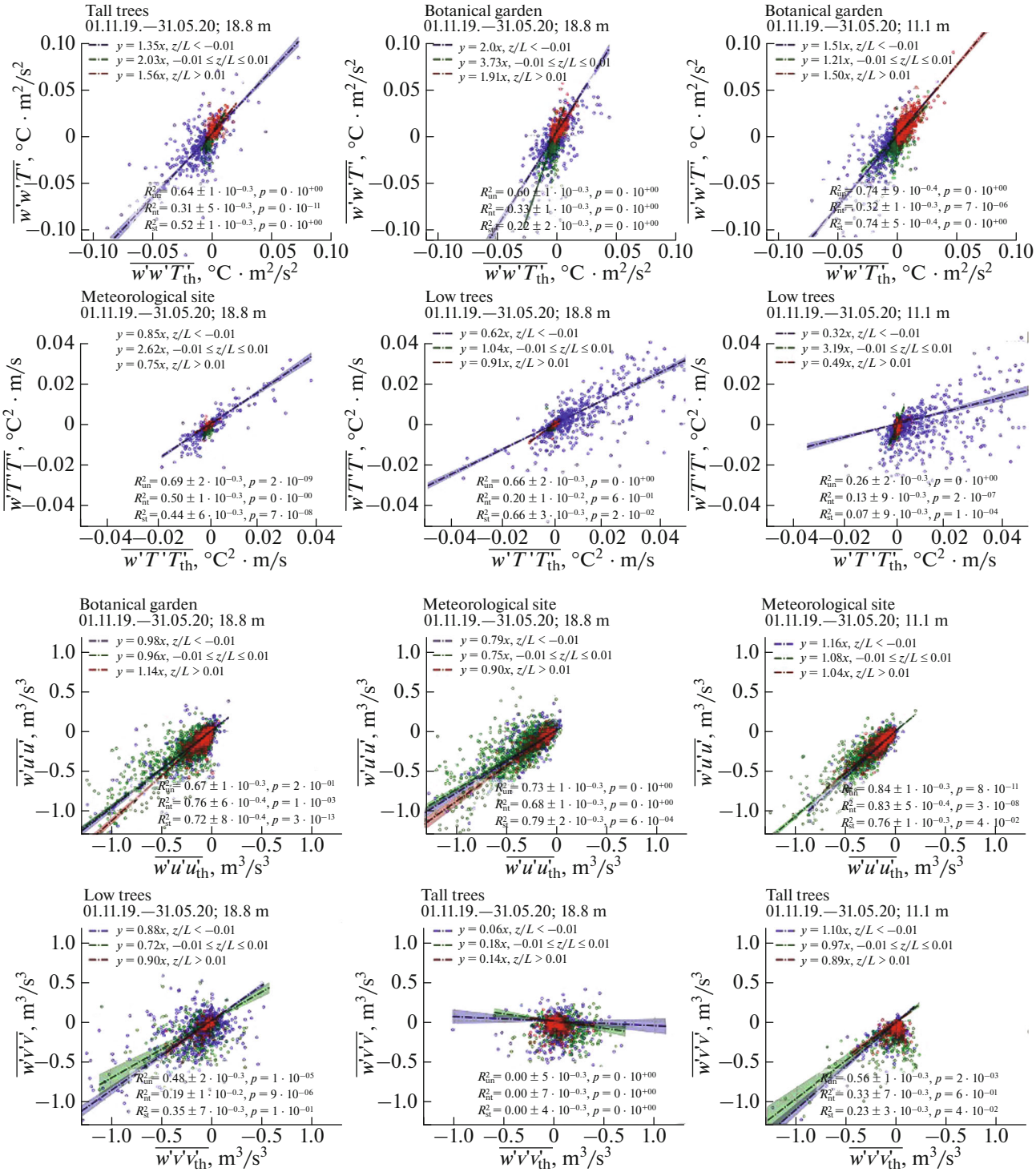

Fig. 3. Distribution of measured third moments $\overline{w'w'T'}$, $\overline{w'T'T'}$, $\overline{w'u'u'}$, $\overline{w'v'v'}$ relative to the theoretical ones at various stratification for wind direction sectors Tall Trees, Botanical Garden, Meteorological Site, and Low Trees according to data at 18.8 (columns 1 and 2) and 11.1 m (column 3). The colored circles show the ratio of the third moments for each 20-min averaging period. Color fill shows confidence intervals. The colors correspond to various conditions of stratification: red is stable, green is neutral, and blue is unstable; stratification is reflected in the legend below with subscripts: st, stable; nt, neutral; un, unstable; and the legend shows the boundaries above definitions of each type of stratification. In the legend, the regression slope (the slope of the dotted lines) is indicated on the top and the determination coefficient and the *p* value are below.

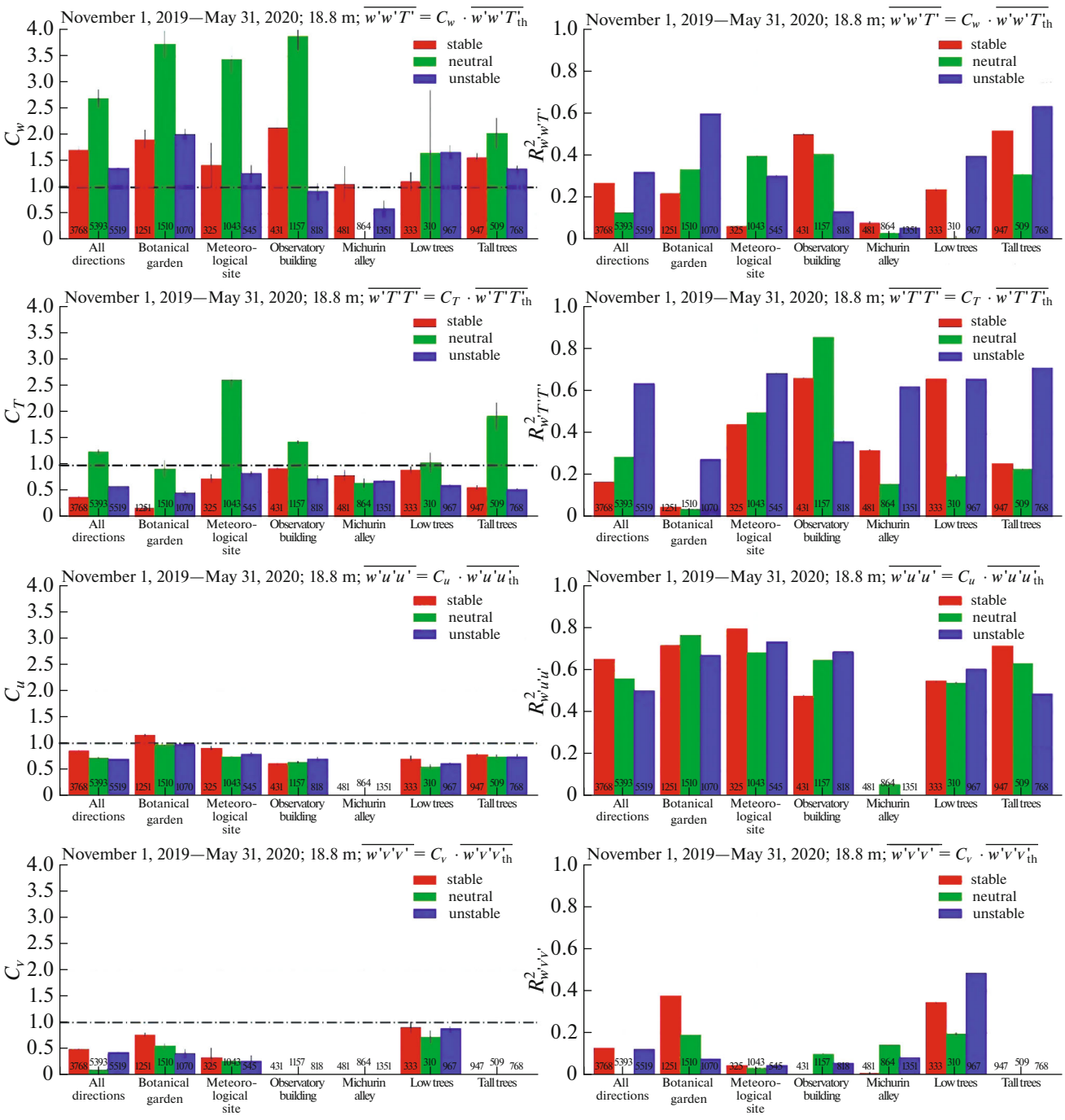

Fig. 4. Slopes (left) and determination coefficients (right) for third moments $\overline{w'w'T'}$ and $\overline{w'T'T'}$, $\overline{w'u'u'}$ and $\overline{w'v'v'}$ according to measurements from November 1, 2019, to May 31, 2020, at a height of 18.8 m for various wind directions (sector names are given in the column captions). The values at the bottom of the columns show the number of cases with a given stratification in a given sector. The black dotted line shows the theoretical regression slope for the third-moment ratio (given in the title for each set of bar graphs). The vertical black lines show the confidence intervals for the values of the coefficients. Colors correspond to different stratification conditions: red is stable, green is neutral, and blue is unstable; stratification is also reflected in the legend.

of accepting hypothesis (1), (2). The lowest values of the determination coefficient are also typical for the conditions of neutral stratification, in 68% of cases, $R^2 < 0.3$, however, in general, third moments $\overline{w'w'T'}$ and $\overline{w'T'T'}$ are characterized by low R^2 values regardless of the stratification conditions; only 29% of the values of the determination coefficients are greater than 0.5. Under unstable and stable stratification, for $\overline{w'w'T'}$ 86% of the C coefficients have a value greater than unity, of which 88% are in the range from 1 to 2,

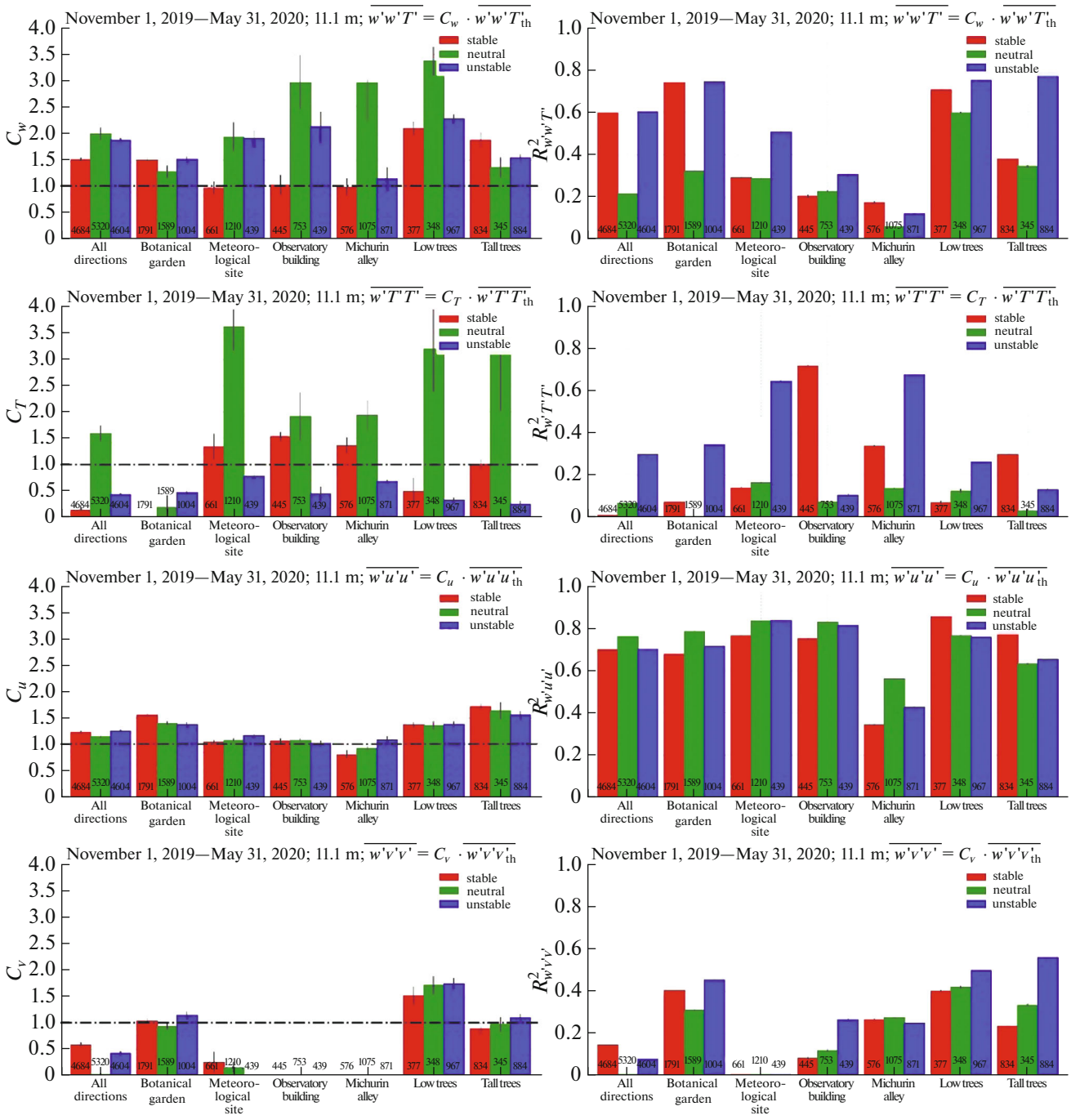

Fig. 5. Slopes (left) and determination coefficients (right) for third moments $\overline{w'w'T'}$ and $\overline{w'T'T'}$, $\overline{w'u'u'}$ and $\overline{w'v'v'}$ according to measurements from November 1, 2019, to May 31, 2020, at a height of 11.1 m for different wind directions (sector names are given in the column captions). The values at the bottom of the columns show the number of cases with a given stratification in a given sector. The black dotted line shows the theoretical regression slope for the third-moment ratio (given in the title for each set of bar graphs). The vertical black lines show the confidence intervals for the values of the coefficients. Colors correspond to different conditions of stratification: red is stable, green is neutral, blue is unstable, and stratification is also reflected in the legend.

and for $\overline{w'T'T'}$, 86% of C values are less than unity, of which 88% are in the range from 0.5 to 1. Under conditions of unstable stratification, hypotheses (1), (2) were confirmed in 100% of cases at 18.8 m and in 71% of cases at 11.1 m, while R^2 for unstable stratification is the highest among other stratification conditions in 75% of cases, which is the best indicator among various stratification conditions for third moments $\overline{w'w'T'}$ and $\overline{w'T'T'}$. This is explained by more favorable conditions for the formation of eddy structures in

an unstable stratified boundary layer, all other things being equal, and thus agrees with the Zilitinkevich hypothesis.

The C and R^2 coefficients for third angular momentum ($\overline{w'u'u'}$, $\overline{w'v'v'}$) within the same sector practically do not differ, from which it follows that the fulfillment of hypothesis (4) is insignificantly affected by the boundary layer stratification conditions. Hypothesis (4) was confirmed for $\overline{w'u'u'}$ in 86% of cases (all sectors except Michurin Alley) at 18.8 m and in 100% of cases at 11.1 m, with an average coefficient of determination greater than 0.6 (with the exception of the Michurin Alley sector at 18.8 m). For third moments $\overline{w'v'v'}$, hypothesis (4) was not confirmed in most cases; only 38% of the C coefficients were in the range from 0.5 to 2, while R^2 does not exceed 0.2 at 18.8 m and 0.3 at 11.1 m in 74% of cases. A significant difference in the coefficients of determination and linear regression obtained for $\overline{w'u'u'}$ and $\overline{w'v'v'}$ is a consequence of the difference in the distributions of these third moments (Fig. 3), on which, in turn, the direction of the prevailing wind in the measurement area affects (Fig. 2). The u axis of acoustic anemometers is directed in the direction of the prevailing flows (southwest) while the v axis is perpendicular to them (southeast) (Fig. 1). Thus, when the wind from the Meteorological Site, Observatory Building, and Tall Trees sectors is practically absent, the wind from the Botanical Garden and Low Trees sectors contains both components and the v component dominates in the wind from the Michurin Alley sector. Thus, it is expected that hypothesis (4) for $\overline{w'u'u'}$ will work poorly in the Michurin Alley sector, as well as in Meteorological Site, Observatory Building, and Tall Trees sectors, for $\overline{w'v'v'}$. However, this reasoning does not completely explain why $\overline{w'v'v'}$ is poorly described by hypothesis (4) in the Michurin Alley sector, and $\overline{w'u'u'}$ is poorly described at 18.8 m and well at 11.1 m in the same sector.

Thus, hypothesis (1) was justified for $\overline{w'w'T'}$ in 76% of cases, hypotheses (2) was justified for $\overline{w'T'T'}$ in 71% of cases, hypotheses (4) was justified for $\overline{w'u'u'}$ in 93% of cases, and hypotheses (4) was justified for $\overline{w'v'v'}$ in 38% of cases. In total, hypotheses (1), (2), and (4) for the tested third moments were confirmed in 70% of cases (80%, except for $\overline{w'v'v'}$).

Note that the statistical methods (Student's t-test, assessment of confidence intervals) used to estimate the reliability of the null hypothesis in most cases refuted the strict formulation of hypothesis (1), (2), (4) about the equality of the measured and theoretical third moments, which can be interpreted as "$C = 1$". However, it should be taken into account that these methods of checking the compliance with the hypothesis of the existing sample are based on the assumption that the distribution of the corresponding random variable is normal. As an illustration of the fact that the distribution of the measured and theoretical third moments does not correspond to the normal one, Fig. 6 presents Q-Q plots (quantile plots), which show the ratio of the quantiles of the normal distribution and the quantiles of the distribution of the third moments that are built based on the full sample for the entire measurement period.

An analysis of the Q-Q plots showed that the empirical distribution of the third moments, both measured and theoretical, has tails many times and, in some cases, an order of magnitude heavier than that of the normal distribution. This is expressed in a significant deviation of the blue line showing the ratio of the quantiles of the normal distribution and the distribution of the third moments from the red straight line indicating the ratio of the quantiles under the condition of the normal distribution of the third moments (Fig. 6). The greatest deviations are observed in the areas of the "extreme" quantiles. In other words, the distribution of the third moments implies a significantly larger number of peak values than the normal one, and therefore, strictly speaking, cannot be described by a normal distribution. This casts doubt on the possibility of using standard statistical tests in the framework of the study of the third moments, assuming the normality of the distribution of the test sample.

In order to obtain a statistical distribution of regression and determination coefficients without relying on the assumption of normality, the bootstrap method (Lahiri, 1999) was used in this study. This method is based on the principle according to which a small subsample (10% of values) is randomly taken from the total amount of available data a large number of times (in our case, 10000), according to which the studied values are calculated, in our case, the angular coefficient of regression and determination, and then the set of values is transformed into a probability density function of the studied characteristics. Figures 7 and 8 show the results of applying the bootstrap method to obtain the probability densities of the C and R^2,coefficients calculated from the ratio of measured and theoretical third moments using data at 11.1 and 18.8 m.

The values of the studied coefficients obtained in the standard calculation do not always coincide with the most probable value obtained by the bootstrap method and are the mathematical expectation of the coefficient. Thus, if the distribution is skewed and has a "heavy tail" in the distribution, the estimate of the desired characteristic obtained by the standard method on the full sample is significantly biased from the most probable value. Figure 7 shows that, under conditions of neutral stratification, the distribution of

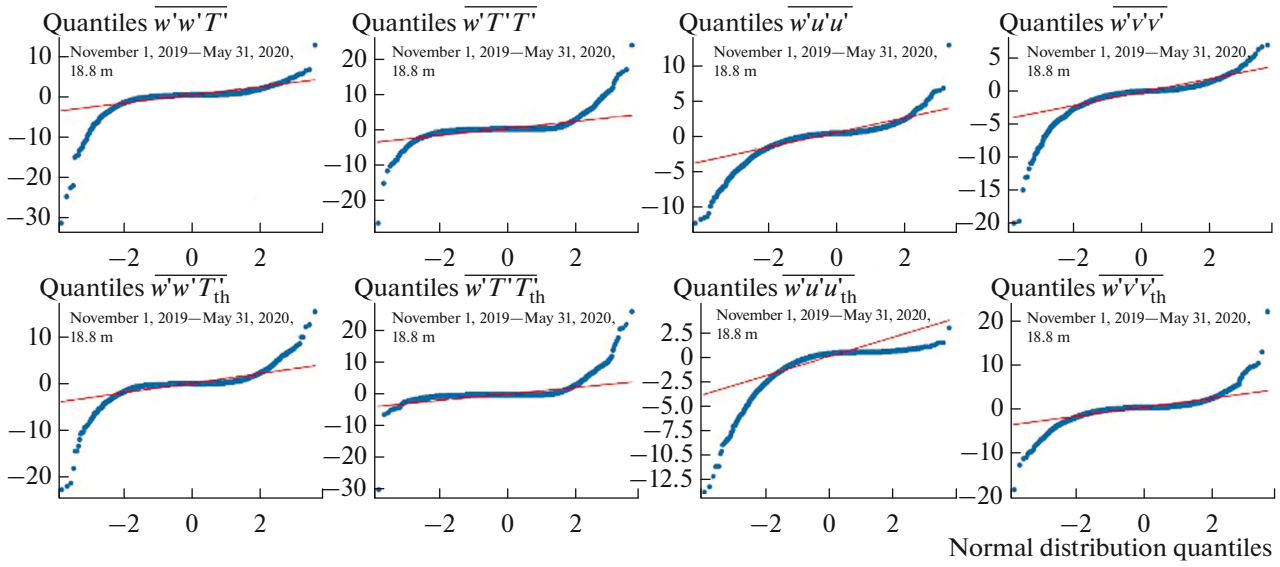

Fig. 6. Plots of standardized quantiles of measured (top row) and theoretical (bottom row) third moments $\overline{w'w'T'}$ and $\overline{w'T'T'}$, $\overline{w'u'u'}$ and $\overline{w'v'v'}$ based on the full data sample with 18.8 m and standard normal distribution quantiles. The red straight line is described by a equation of $y = x$ and shows the absolute coincidence of the distribution of the studied quantity with the normal distribution. The blue curve shows the actual ratio of the distribution of the third moments and the normal distribution.

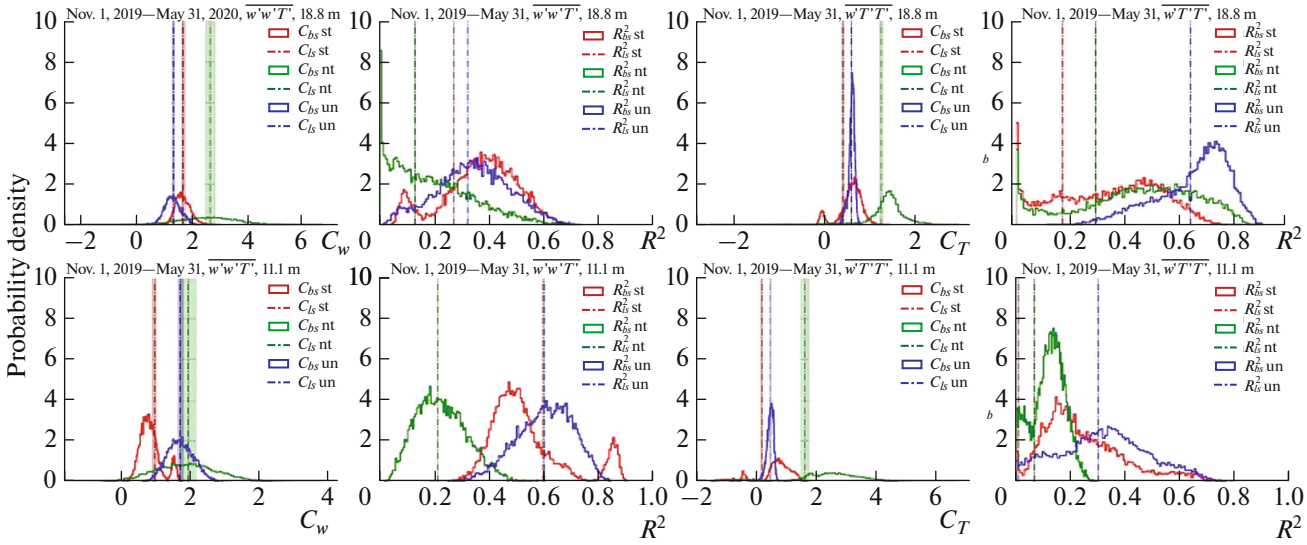

Fig. 7. Distribution densities of regression slopes (columns 1 and 3) and determination coefficients (columns 2 and 4) obtained by the bootstrap method (colored lines, subscript "bs" in the legend), and values of regression slopes and determination coefficients (colored dotted lines) with confidence intervals (color fill) that are obtained based on the full sample (from November 1, 2019, to May 31, 2020) by the standard method (the subscript "ls" in the legend), for third moments $\overline{w'w'T'}$ (columns 1 and 2), $\overline{w'T'T'}$ (columns 3 and 4), at a height of 18.8 (top row) and 11.1 m (bottom row). The colors correspond to different conditions of stratification: red is stable, green is neutral, blue is unstable and the stratification is reflected in the legend by subscripts: st, stable; nt, neutral; and un, unstable.

the regression slope for third moments $\overline{w'w'T'}$ and $\overline{w'T'T'}$ practically does not have a peak and, on average, is quasi-uniform distributed in the range from −1 to 4. In this case, the distribution of R^2 for the ratio of the same moments with neutral stratification has a peak in the range from 0 to 0.3. This indicates a high degree of unreliability of the C, coefficients obtained using linear approximation, which can be interpreted in terms of the Zilitinkevich hypothesis as the absence

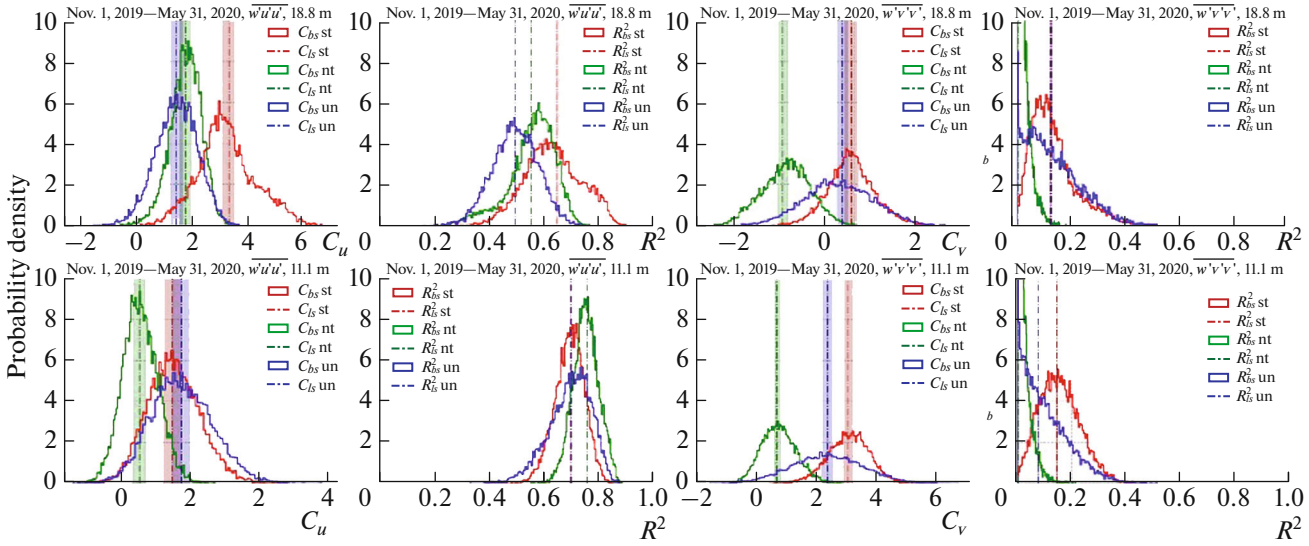

Fig. 8. Distribution densities of regression slopes (columns 1 and 3) and determination coefficients (columns 2 and 4) obtained by the bootstrap method (colored lines, subscript "bs" in the legend) and values of regression slopes and determination coefficients (color dotted lines) with confidence intervals (color fill) that are obtained based on the full sample (from November 1, 2019, to May 31, 2020) by the standard method (in the legend subscript "ls"), for third moments $\overline{w'u'u'}$ (columns 1 and 2) and $\overline{w'v'v'}$ (columns 3 and 4), at a height of 18.8 (top row) and 11.1 m (bottom row). The colors correspond to different conditions of stratification: red is stable, green is neutral, and blue is unstable; stratification is reflected in the legend by subscripts: st, stable; nt, neutral; and un, unstable.

of large coherent structures under conditions of a neutrally stratified boundary layer. In contrast, under conditions of unstable stratification, for third moments $\overline{w'w'T'}$ and $\overline{w'T'T'}$ $\overline{w'T'T'}$, there are clearly pronounced peaks in the distribution of slope coefficients (especially for) that are in the ranges from 0 to 2. This indicates the statistical significance of the estimates of the C coefficient. The maxima of probability densities of R^2 under unstable stratification are shifted towards higher values of determination coefficients relative to other types of stratification, which together confirms the earlier conclusion that relations (1) and (2) are best satisfied under conditions of unstable stratification.

The distributions of the regression and determination coefficients for the third moments $\overline{w'u'u'}$ and $\overline{w'v'v'}$ are fundamentally different from each other (Fig. 7). For example, the regression slopes $\overline{w'u'u'}$ for all types of stratification have an extremely high probability density. All values are distributed in the range from 0.4 to 1.1 at 18.8 m and from 1 to 1.5 at 11.1 m with clearly expressed symmetrical peaks. The average coefficients of determination $\overline{w'u'u'}$ for all types of stratification are greater than 0.5. For the level of 11.1 m, more than 90% of the R^2values are in the range from 0.6 to 0.8, which makes it possible to conclude that relation (4) is valid with respect to third moments $\overline{w'u'u'}$. The opposite situation is observed for third moments $\overline{w'v'v'}$, the distributions of the regression coefficients do not have a pronounced peak; and, although the average values for the cases of unstable and stable stratification lie on the lower boundary of the conformity of the tested hypothesis, more than 50% of all C values are less than 0.5. In this case, 99% of the determination coefficient values for all stratification conditions are less than 0.4 with peaks in the distribution less than 0.2, which confirms the extremely low correlation of third moments $\overline{w'v'v'}$ and the absence of a pronounced linear trend in their distribution, which is also shown in Fig. 3.

CONCLUSIONS

In this study, for the first time, using a long time series of data (from November 1, 2019, to May 31, 2020), the algebraic dependence of moments of different orders suggesting the presence of organized turbulent structures was confirmed under conditions of various stratification over a surface of complex geometric shape. For the first time, the validity of the Zilitinkevich hypothesis in the statistical sense was demonstrated for the third moments of the velocity components.

Here we demonstrated that the statistical distribution of the third moments does not correspond to a normal distribution, so the standard methods for estimating the reliability of hypotheses regarding these moments (Student's test and estimation of confidence intervals) are not sufficiently substantiated. The use of the bootstrap method makes it pos-

sible to obtain more detailed statistical information about the parameters of the diagnostic relation of turbulent moments of various orders and take into account the features of the empirical distribution of the studied characteristics. The analysis of the probability density functions of the linear regression and determination coefficients obtained by the bootstrap method confirmed the conclusions made based on the regression analysis.

The diagnostic relation of the third and second moments according to the Zilitinkevich hypothesis (Zilitinkevich et al., 1999; Abdella and McFarlane, 1997) for temperature ($\overline{w'w'T'}$, $\overline{w'T'T'}$) and momentum components ($\overline{w'u'u'}$, $\overline{w'v'v'}$) was established to be fulfilled over the urban surface in 70% of cases with values of the dimensionless constant from 0.5 to 2 (in 80% with no allowance for $\overline{w'v'v'}$). The statistical significance and parameters of diagnostic formulas for third moments $\overline{w'w'T'}$ and $\overline{w'T'T'}$ depend on the stratification conditions, while for $\overline{w'u'u'}$ and $\overline{w'v'v'}$ they depend on the direction of the prevailing wind. No dependence on the nature of the underlying surface was estaballlished. The most accurately discussed hypothesis describes the relation of the third and second moments for $\overline{w'u'u'}$, this relation is observed in 93% of cases with average $R^2 > 0.6$ (except for the sector oriented perpendicular to the u component of the wind velocity), while $\overline{w'v'v'}$ is weakly described by a linear regression model with a unit regression slope. For third moments $\overline{w'w'T'}$ and $\overline{w'T'T'}$, there was a tendency to overestimate the C coefficient at neutral stratification relative to other stratification conditions in of 78% of cases. Under conditions of stable and unstable stratification, the values of the C coefficient most often are in the range from 1 to 2 for $\overline{w'T'T'}$ and in the range from 0.5 to 1 for $\overline{w'T'T'}$. For $\overline{w'w'T'}$, $\overline{w'T'T'}$ the most strictly studied relation is satisfied under conditions of unstable stratification.

FUNDING

This work was partially supported by the Ministry of Science and Higher Education of Russian Federation, agreement nos. 075-15-2021-574 (technical support for measurements) and 075-15-2022-284 (analysis of the results of statistical data processing). Statistical data processing was supported by the Russian Science Foundation, grant no. 21-17-00249.

CONFLICT OF INTEREST

The authors declare that they have no conflicts of interest.

REFERENCES

Abdella, K. and McFarlane, N., A new second-order turbulence closure scheme for the planetary boundary layer, *J. Atmos. Sci.*, 1997, vol. 54, no. 14, pp. 1850–1867.

Artamonov, A.Yu., Varentsov, M.I., Gavrikov, A.V., Pashkin, A.D., Repina, I.A., and Stepanenko, V.M., The micrometeorological tower of the Moscow State University Meteorological Observatory, in *Ekologo-klimaticheskie kharakteristiki atmosfery Moskvy v 2018 g. po dannym Meteorologicheskoi observatorii MGU imeni M.V. Lomonosova* (Ecological and Climatic Characteristics of the Moscow Atmosphere in 2018 According to Data from the Meteorological Observatory of the Moscow State University), Moscow, 2019, pp. 157–161.

Barskov, K.V., Glazunov, A.V., Repina, I.A., Stepanenko, V.M., Lykosov, V.N., and Mammarella, I., On the applicability of similarity theory for the stable atmospheric boundary layer over complex terrain, *Izv., Atmos. Ocean. Phys.*, 2018, vol. 54, no. 5, pp. 462–471.

Barskov, K., Stepanenko, V., Repina, I., Artamonov, A., and Gavrikov, A., Two regimes of turbulent fluxes above a frozen small lake surrounded by forest, *Boundary Layer Meteorol.*, 2019, vol. 173, no. 3, pp. 311–320.

Barskov, K., Chechin, D., Drozd, I., Artamonov, A., Pashkin, A., Gavrikov, A., Stepanenko, V., Varentsov, M., and Repina, I., Relationships between second and third moments in the surface layer under different stratification over grassland and urban landscapes, *Boundary Layer Meteorol.*, 2022, pp. 1–28.

Drozd, I., Gavrikov, A., and Stepanenko, V., Comparative characteristics of gap filling methods in high-frequency data of micrometeorological measurements, *IOP Conf. Ser.: Earth Environ. Sci.*, 2022a, vol. 1023, no. 1, p. 012009.

Drozd, I., Repina, I., Gavrikov, A., Stepanenko, V., Artamonov, A., Pashkin, A., and Varentsov, A., Atmospheric turbulence structure above urban nonhomogeneous surface, *Russ. J. Earth Sci.*, 2022b, vol. 22, no. 5, p. 12.

Grachev, A.A., Andreas, E.L., Fairall, C.W., Guest, P.S., and Persson, P.O.G., Similarity theory based on the Dougherty–Ozmidov length scale, *Q. J. R. Meteorol. Soc.*, 2015, vol. 141, no. 690, pp. 1845–1856.

Grachev, A.A., Leo, L.S., Fernando, H.J.S., Fairall, C.W., Creegan, E., Blomquist, B.W., Christman, A.J., and Hocut, C.M., Air–sea/land interaction in the coastal zone, *Boundary Layer Meteorol.*, 2018, vol. 167, no. 2, pp. 181–210.

Johansson, C., Smedman, A-S., Högström, U., Brasseur, J.G., and Khanna, S., Critical test of the validity of Monin–Obukhov similarity during convective conditions, *J. Atmos. Sci.*, 2001, vol. 58, no. 12, pp. 1549–1566.

Kadivar, M., Tormey, D., and McGranaghan, G., A review on turbulent flow over rough surfaces: Fundamentals and theories, *Int. J. Thermofluids*, 2021, vol. 10, p. 100077.

Kaimal, J.C. and Finnigan, J.J., *Atmospheric Boundary Layer Flows: Their Structure and Measurement*, Oxford: Oxford University Press, 1994.

Lahiri, S.N., Theoretical comparisons of block bootstrap methods, *Ann. Stat.*, 1999, vol. 27, pp. 386–404.

Monin, A.S. and Obukhov, A.M., Main regularities of turbulent mixing in the atmospheric surface layer, *Tr. GEOFIAN*, 1954, no. 24, pp. 163–187.

Monin, A.S. and Yaglom, A.M., *Statisticheskaya gidromekhanika* (Statistical Hydromechanics), vol. 1, Moscow: Nauka, 1965; vol. 2, Moscow: Nauka, 1967.

Pashkin, A.D., Repina, I.A., Stepanenko, V.M., Bogomolov, V.Yu., Smirnov, S.V., and Tel'minov, A.E., Relationship of statistical characteristics of turbulence with coherent structures based on the results of pulsation measurements in an urban canyon, *Protsessy Geosredakh*, 2021, no. 1, pp. 1020–1027.

Stiperski, I. and Calaf, M., Generalizing Monin–Obukhov similarity theory (1954) for complex atmospheric turbulence, 2022. https://arxiv.org/abs/2206.14592.

Tong, C. and Nguyen, K.X., Multipoint Monin–Obukhov similarity and its application to turbulence spectra in the convective atmospheric surface layer, *J. Atmos. Sci.*, 2015, vol. 72, pp. 4337–4348.

Wilson, J.D., Monin–Obukhov functions for standard deviations of velocity, *Boundary-Layer Meteorol.*, 2008, vol. 129, no. 3, pp. 353–369.

Wyngaard, J.C., *Turbulence in the Atmosphere*, New York: Cambridge University Press, 2010.

Zilitinkevich, S.S., Third-order transport due to internal waves and non-local turbulence in the stably stratified surface layer, *Q. J. R. Meteorol. Soc.*, 2002, vol. 128, no. 581, pp. 913–925.

Zilitinkevich, S., Gryanik, V., Lykossov, V., and Mironov, D., Third-order transport and nonlocal turbulence closures for convective boundary layers, *J. Atmos. Sci.*, 1999, vol. 56, pp. 3463–3477.

Translated by A. Ivanov